ISSN 1068-3356, Bulletin of the Lebedev Physics Institute, 2017, Vol. 44, No. 2, pp. 46–49. © Allerton Press, Inc., 2017.
Original Russian Text © V.S. Gorelik, A.D. Kudryavtseva, M.V. Tareeva, N.V. Tcherniega, A.I. Vodchits, 2017, published in Kratkie Soobshcheniya po Fizike, 2017, Vol. 44, No. 2, pp. 30–36.

Multifrequency Stimulated Raman Scattering of Light in Liquid Nitrogen Infiltrated into 3D Photonic Crystals

V. S. Gorelik[a], A. D. Kudryavtseva[a], M. V. Tareeva[a], N. V. Tcherniega[a], and A. I. Vodchits[b]

[a] *Lebedev Physical Institute, Russian Academy of Sciences, Leninskii pr. 53, Moscow, 119991 Russia; e-mail: gorelik@sci.lebedev.ru*
[b] *Stepanov Institute of Physics, National Academy of Sciences, pr. Nezavisimosti 68, Minsk, 220072 Belarus*

Received July 7, 2015

Abstract—Spectral characteristics of stimulated Raman scattering at least in synthetic opal matrices infiltrated with liquid nitrogen upon excitation by nanosecond laser pulses are studied. The effect of the stop band position on the generation efficiency of anti-Stokes components of stimulated Raman scattering up to the third order is demonstrated. The excitation threshold of stimulated Raman scattering in liquid nitrogen infiltrated into opals is significantly lower in comparison with the generation in bulk samples.

DOI: 10.3103/S1068335617020051

Keywords: stimulated Raman scattering of light, liquid nitrogen, photonic crystal, stop band.

Introduction. Stimulated Raman scattering of light (SRS) in liquid nitrogen was studied in many works [1–5]. In [1], up to 6 Stokes and to 8 anti-Stokes SRS components were observed. The number of observed components depended on the pump beam focusing sharpness: the number of components increased with a decrease in the focal length of the lens focusing exciting radiation to a material. It was shown experimentally that the intensity of anti-Stokes components decreases with increasing their frequency. SRS was excited from the pump energy of ~20 mJ at the pulse duration of 20 ns [1, 3]; however, significant conversion factors were achieved at substantially higher pump energies (> 2.5 J in [1] and > 0.5 J in [3]). Furthermore, to achieve high conversion factors of laser radiation in SRS, cells several cm long should be used (as a rule, cells from 50 to 150 mm long were used in experiments).

To solve the problems of increasing the efficiency of nonlinear-optical processes, the use of structures with permittivity modulation on the scale comparable with the electromagnetic pump radiation wavelength is optimum [6, 7].

The nonlinear optical interaction of light and materials in such structures is enhanced due to a high density of photon states at photonic band gap (PBG) edges.

Recently, an SRS excitation technique based on introducing an active medium into structures with PBG was developed. In particular, efficient SRS amplification in porous photon waveguides filled with inert gases [8–10] and in molecular liquids introduced into pores of colloidal photonic crystals [11, 12] is widely used.

Colloidal photonic crystals representing a structure consisting of close-packed silicon dioxide globules (synthetic opal matrices) are promising materials for nonlinear optics [6, 7]. The efficiency of the pump wave conversion to a scattered wave can be significantly increased in such structures, and the excitation threshold of stimulated light scattering can be lowered [12, 13].

Despite the fact that the complete photonic band gap in synthetic opal matrices does not exist (mainly due to the small refractive index contrast), and only the stop band exists, which sets a preferential direction in which the propagation of electromagnetic radiation of a certain frequency range is forbidden, it is convenient to use opal matrices, filling interstices between silicon dioxide globules with various Raman-active materials.

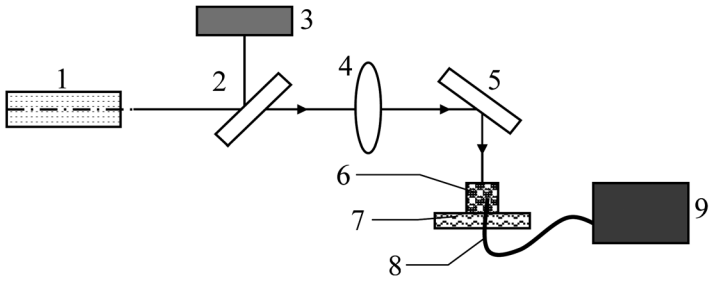

Fig. 1. Schematic of the setup for observing forward SRS: (1) ruby laser, (2) rotating quartz plate, (3) system for measuring excitation beam parameters, (4) system of lenses focusing the exciting beam to the sample, (5) mirror, (6) sample, (7) liquid nitrogen cell, (8) optical waveguide, and (9) spectrometer.

Proven technologies of the production of synthetic opal matrices allow preparation of the samples with a typical silicon dioxide globule size of 200–700 nm. Due to submicrometer globule sizes, stop bands in the visible spectral region are formed in these structures.

Using matrices with various sphere sizes and varying the sample illumination geometry, the stop band parameters (its spectral position and contrast) can be controlled to increase the efficiency of various nonlinear processes, including SRS.

Experiment. The schematic of the setup used to observe SRS in liquids is shown in Fig. 1.

As an exciting radiation source, a single-pulse ruby laser (1) operating in the Q-switching mode was used in the experiment for observing SRS in liquid nitrogen. The lasing wavelength was 694.3 nm, the lasing pulse duration at half height $\tau = 20$ ns, the maximum pulse energy was 0.4 J, the beam divergence was $3.5 \cdot 10^{-4}$ rad, and the spectral lasing line width was 0.015 cm^{-1}.

The lattice constant of synthetic opal controlled by the silicon dioxide globule diameter was from 180 to 350 nm for various samples.

With varying the globule diameter and the filling factor of synthetic opal with liquid nitrogen, the sample stop band position varied according to the dependence

$$\lambda_{\mathrm{PBG}} = 2D\sqrt{2/3}n_{\mathrm{eff}}\cos\theta, \tag{1}$$

where n_{eff} is the effective refractive index in the crystal, depending on the degree of sample infiltration, and θ is the angle of light incidence on the periodic structure.

Typical reflectance spectrum of the synthetic opal sample used in the experiment is shown in Fig. 2. The maximum in the reflectance spectrum corresponds to the stop band center position, $\lambda_{\mathrm{PBG}} =$ 622 nm. The band width is $\Delta\lambda_{\mathrm{PBG}} \approx 70$ nm.

Experimental results. In this series of experiments on pulsed laser radiation scattering in synthetic opal matrices infiltrated with liquid nitrogen, the forward SRS was observed. Figure 3 shows the SRS spectrum in liquid nitrogen infiltrated into synthetic opal normalized to the maximum intensity.

To study the dependences of the SRS generation efficiency in liquid nitrogen on the morphology of synthetic opal infiltrated with nitrogen, we used opal matrix samples with various globule diameters and, hence, different stop band positions.

The effect of liquid nitrogen nanostructuring on SRS generation is illustrated in Fig. 4. In case (a), the first and second anti-Stokes components appear at stop band edges and are significantly amplified. The first anti-Stokes SRS component of liquid nitrogen appears at the long-wavelength edge δ_+ of the photonic band gap of this photonic crystal ($\lambda_{+1} = 598$ nm $\in \delta_+(\lambda_{\mathrm{PBG}})$), and the second anti-Stokes component appears at the short-wavelength edge $\delta_-(\lambda_{+2} = 526$ nm $\in \delta_-(\lambda_{\mathrm{PBG}}))$.

In case (b), the first anti-Stokes SRS component is suppressed, since it appears in the stop band of this crystal sample (the crystal globule diameter is $D = 280$ nm, the stop band position is $\lambda_{\mathrm{PBG}} =$ 600 nm, and the stop band width is ~70 nm).

It should be noted that the partial effect of synthetic opal on SRS generation in liquid also consists in an increase in the efficiency of laser radiation conversion to SRS by 5–6% due to local (periodically arranged) fields which being bent at the liquid–SiO_2 globule interface, contribute to the photon–phonon interaction enhancement [14].

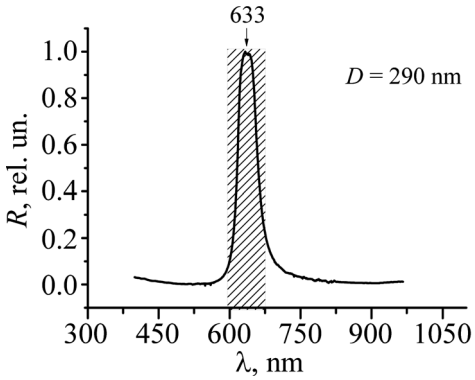

Fig. 2. Reflectance spectrum of the three-dimensional synthetic opal sample with silicon dioxide globule diameter $D = 290$ nm at normal radiation incidence on the sample. The shaded area corresponds to the photonic band gap in the sample.

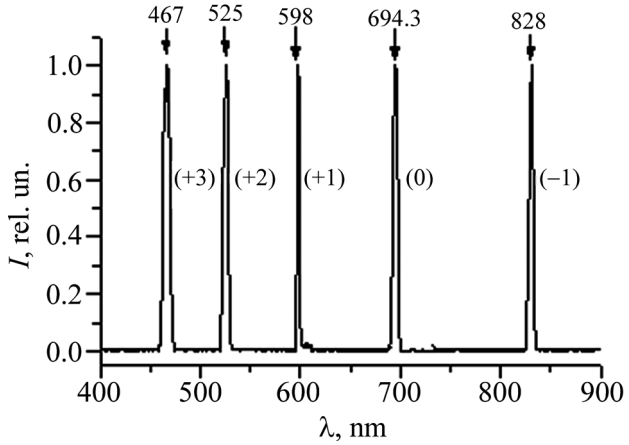

Fig. 3. SRS spectrum in liquid nitrogen infiltrated into the synthetic opal matrix with a globule diameter of 260 nm. The intensity of components is normalized to the maximum intensity. Notations (+3), (+2), (+1) correspond to the third, second, and first anti-Stokes components, respectively, (0) is the exciting laser radiation line, and (-1) is the first Stokes component.

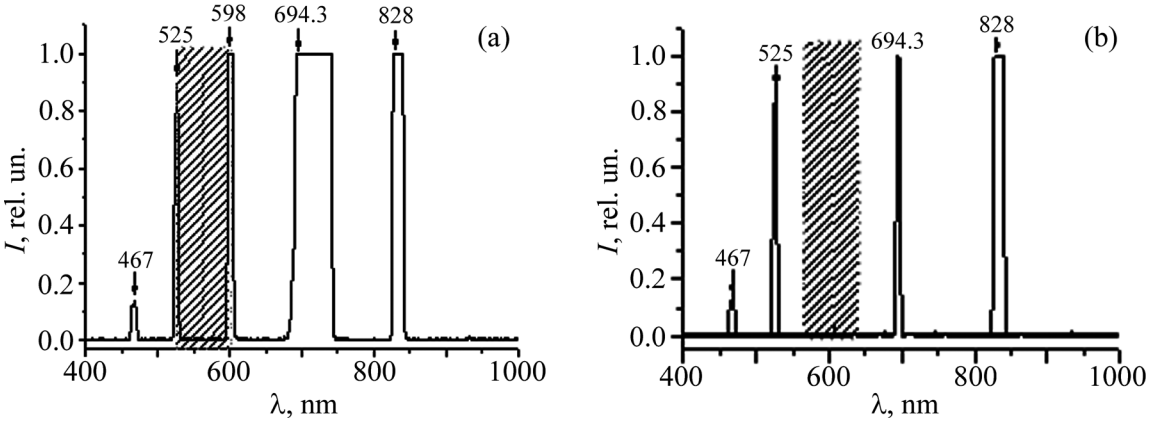

Fig. 4. Effect of the synthetic opal structure on forward SRS generation in liquid nitrogen: (a) the first and second anti-Stokes components are amplified being appeared at stop band edges (shaded area) of synthetic opal with globule diameter $D = 450$ nm, (b) the first anti-Stokes component appears at the stop band of synthetic opal with globule diameter $D = 310$ nm and is suppressed.

Discussion. The anti-Stokes generation of forward SRS components in liquid nitrogen introduced into pores of the three-dimensional photonic crystal, i.e., synthetic opal, achieved in this study, became possible in the samples in which the frequencies of exciting radiation and SRS components appeared at the photonic stop band edges. To generate individual components, synthetic opals with such stop band characteristics (position and width) at which this condition is satisfied were selected. This suggests that the generation process in this case is not completely parametric.

Conclusions. It was found that the introduction of liquid nitrogen into synthetic opal pores causes a decrease in the SRS generation threshold upon excitation by giant ruby laser pulses. Thus, it became possible to observe the anti-Stokes components of the first, second, and third order with the conversion efficiency to 40%.

This method for generating the highest anti-Stokes components seems significantly less laborious in comparison with methods for generating anti-Stokes SRS components of higher orders in photon waveguides filled with gases.

This study offers the possibility of multifrequency conversion of laser radiation of the visible region to the ultraviolet region of the spectrum.

The high destruction threshold of the synthetic opal sample infiltrated with liquid nitrogen offers prospects for the use of opal matrices for irradiation with high-intensity excitation sources such as pulsed lasers of picosecond (20–30 ps) duration with a large repetition rate, providing laser radiation power densities in the sample to 1 TW/cm^2.

ACKNOWLEDGMENTS

This study was supported by the Russian Foundation for Basic Research (RFBR) and the Belarusian Republican Foundation for Fundamental Research (BRFFR) (RFBR project no. 16-32-60026-mol-a-dk and joint project of RFBR and BRFFR RFBR-BRFFR no. 16-52-00026-Bel-a (BRFFR-RFBR F16R-063)).

REFERENCES

1. V. V. Ragul'skii and F. S. Faizullov, JETP Lett. **6**, 887 (1967).
2. J. B. Grun, A. K. McQuillan, and B. P. Stoicheff, Phys Rev **180**, 179 (1969).
3. A. D. Kudryavtseva, A. I. Sokolovskaya, and M. M. Sushchinskii, Zh. Eksp. Teor. Fiz. **59**, 1556 (1971) [Sov. Phys. JETP **32**, 849 (1971)].
4. S. R. J. Brueck and H. Kildal, IEEE J. Quantum Electron. QE-18, 310 (1982).
5. N. Tcherniega, A. Sokolovskaya, A. D. Kudryavtseva, et al., Opt. Commun. **181**, 197 (2000).
6. M. Bertolotti, J. Opt. A: Pure Appl. Opt. **8**, S9 (2006).
7. V. S. Gorelik, N. V. Tcherniega, and A. D. Kudryavtseva, J. Russ. Laser Res. **29**, 551 (2008).
8. P. St. J. Russell, P. Hölzer, W. Chang, et al., Nat. Photonics **8**, 278 (2014).
9. F. Couny, F. Benabid, and O. Carraz, J. Opt. A: Pure Appl. Opt. **9**, 156 (2007).
10. Takayuki Suzuki, Masataka Hirai, and Masayuki Katsuragawa, Phys. Rev. Lett. **101**, 243602 (2008).
11. V. S. Gorelik, A. D. Kudryavtseva, V. A. Orlovich, et al., J. Russ. Laser Res. **32**, 277 (2011).
12. V. S. Gorelik, A. D. Kudryavtseva, M. V. Tareeva, and N. V. Tcherniega, Neorg. Mater. **50**, 1219 (2014). [Inorg. Mater. **50**, 1217 (2014).]
13. V. S. Gorelik, A. D. Kudryavtseva, N. V. Tcherniega, et al., J. Russ. Laser Res. **34**, 50 (2013).
14. H. A. Sumeruk, S. Kneip, D. R. Symes, et al., Phys. Rev. Lett. **98**, 045001 (2007).